Supporting Information

Site-Specific Internal Motions in GB1 Protein Microcrystals Revealed by 3D ^{2}H-^{13}C-^{13}C Solid-State NMR Spectroscopy

Xiangyan Shi, Chad M. Rienstra*

Department of Chemistry, University of Illinois at Urbana−Champaign, 600 South Mathews Avenue, Urbana, Illinois 61801, United States

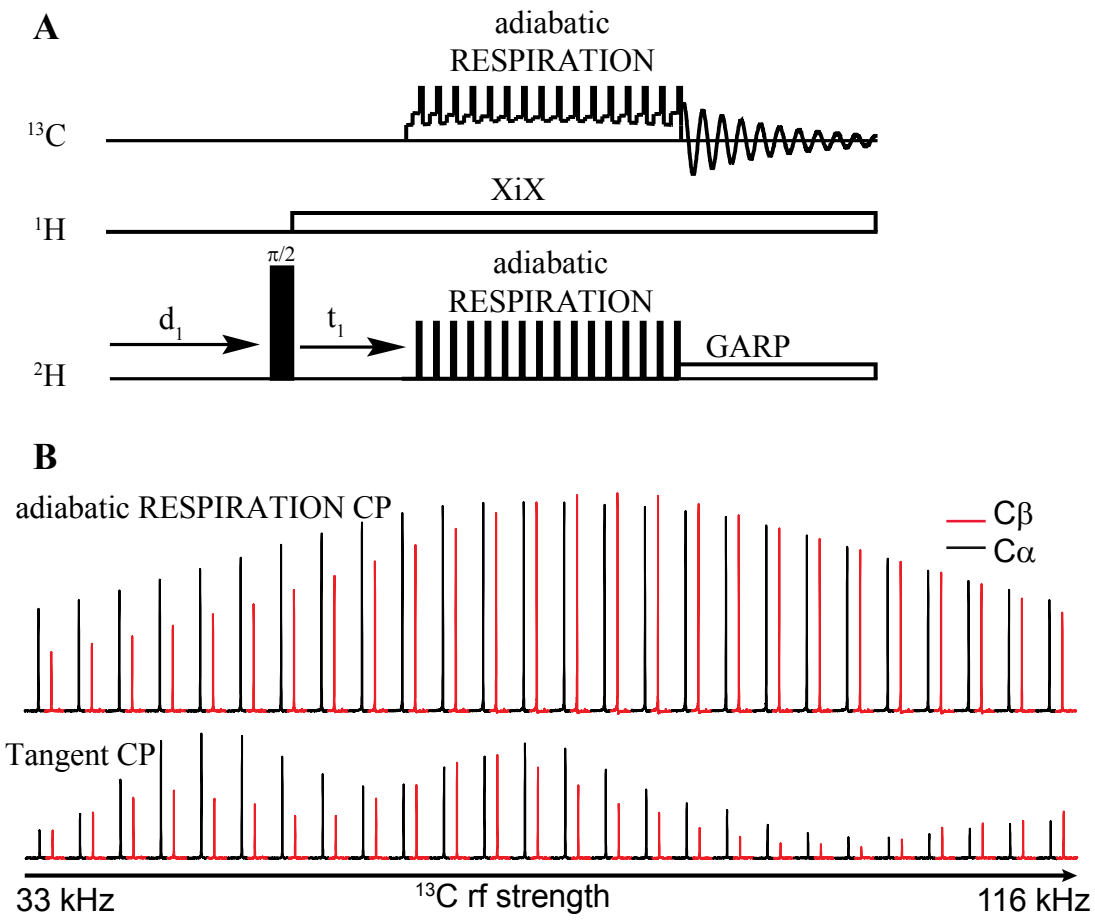

Figure S1. (A) 2D ^{2}H-^{13}C adiabatic RESPIRATION CP solid-state NMR pulse sequence. (B) Adiabatic RESPIRATION and Tangent CP matching profiles shown by a series of 1D spectra (t_1 = 0) acquired with various spin-lock rf field strength. Data was collected on U-[$^{13}C_3$,$^{2}H_4$,^{15}N] Ala crystalline powder. The detected Ala Cα and Cβ are presented. ^{2}H spin-lock rf field strength was fixed at 83 kHz and ^{13}C spin-lock rf field strength was arrayed from 33 kHz to 116 kHz with a constant step of 3.2 kHz. The CP contact time is 1 ms in both cases.

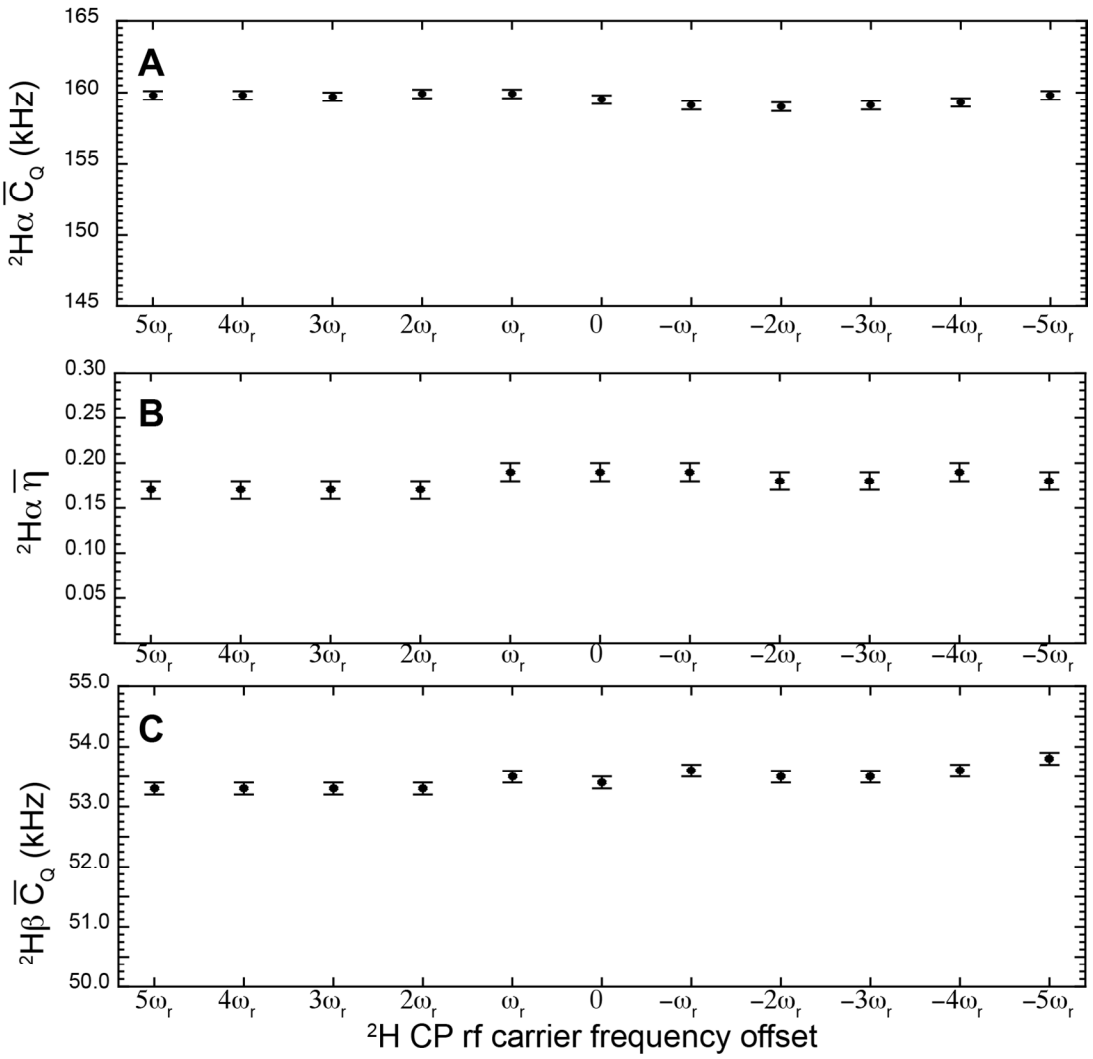

Figure S2. (A) Ala ^{2}Hα $\overline{C_Q}$, (B) ^{2}Hα $\overline{\eta}$ and (C) ^{2}Hβ $\overline{C_Q}$ extracted from 2D ^{2}H-^{13}C adiabatic RESPIRATION CP experiments with different ^{2}H CP rf carrier frequency offsets. Data was collected on U-[$^{13}C_3$,$^2H_4$,^{15}N] Ala crystalline powder. ^{2}H CP rf carrier offset was set to n*ω_r (n = 0, ±1, ±2, ±3, ±4, ±5 and ω_r = 22.222 kHz. 86 kHz ^{2}H and 76 kHz ^{13}C spin-lock rf field strengths and 1 ms contact time were used for adiabatic RESPIRATION CP magnetization transfer. Fitting was performed with DMFit package[1] and fits are shown in Figure S3.

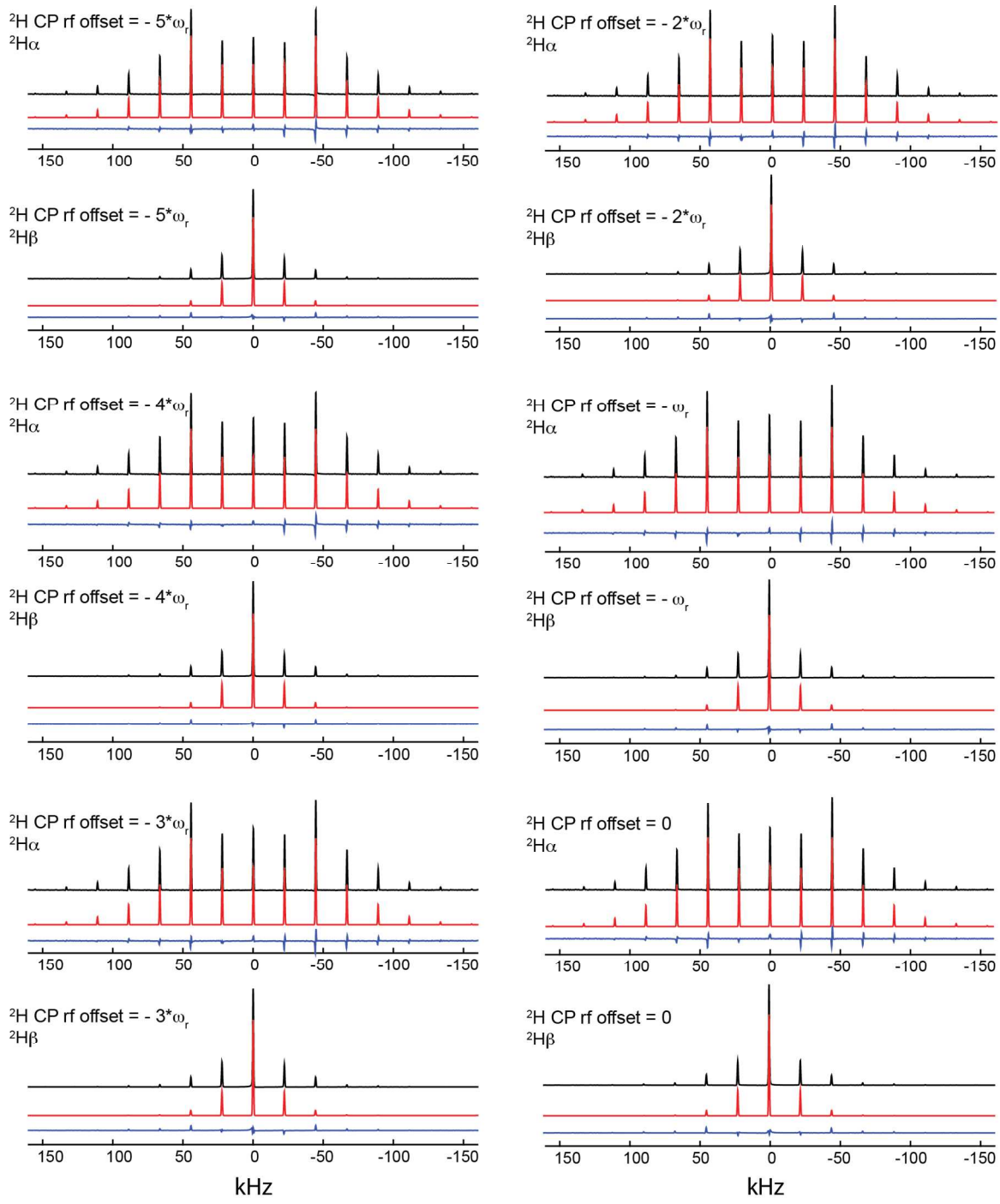

Figure S3. Fits of Ala ^{2}H line shapes extracted from 2D ^{2}H-^{13}C adiabatic RESPIRATION CP experiments with different ^{2}H CP rf carrier frequency offsets. Experimental data (black), fits (red) and residuals (blue) are displayed. Experimental details and fitting results were shown in Figure S2.

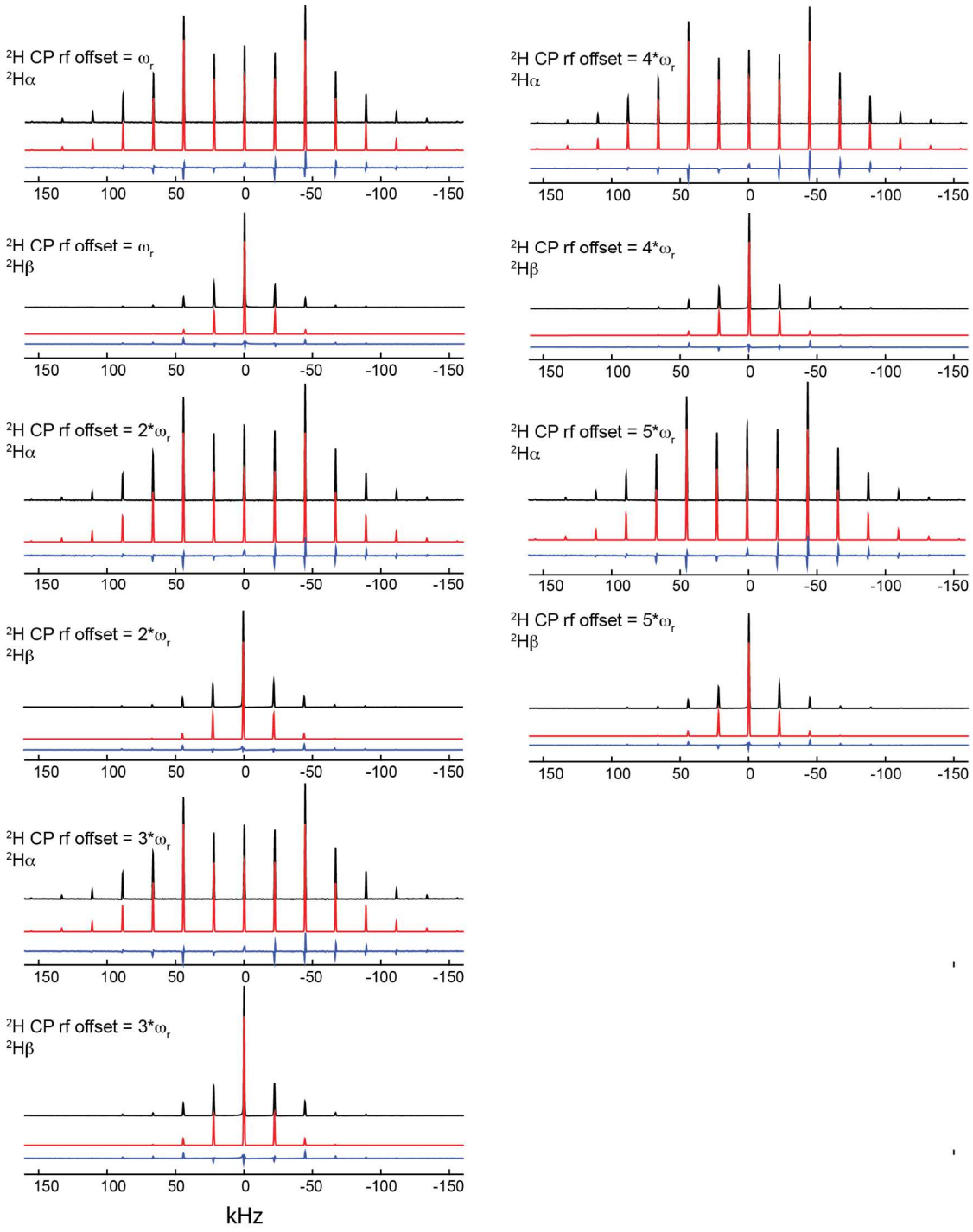

Figure S3 (Continued)

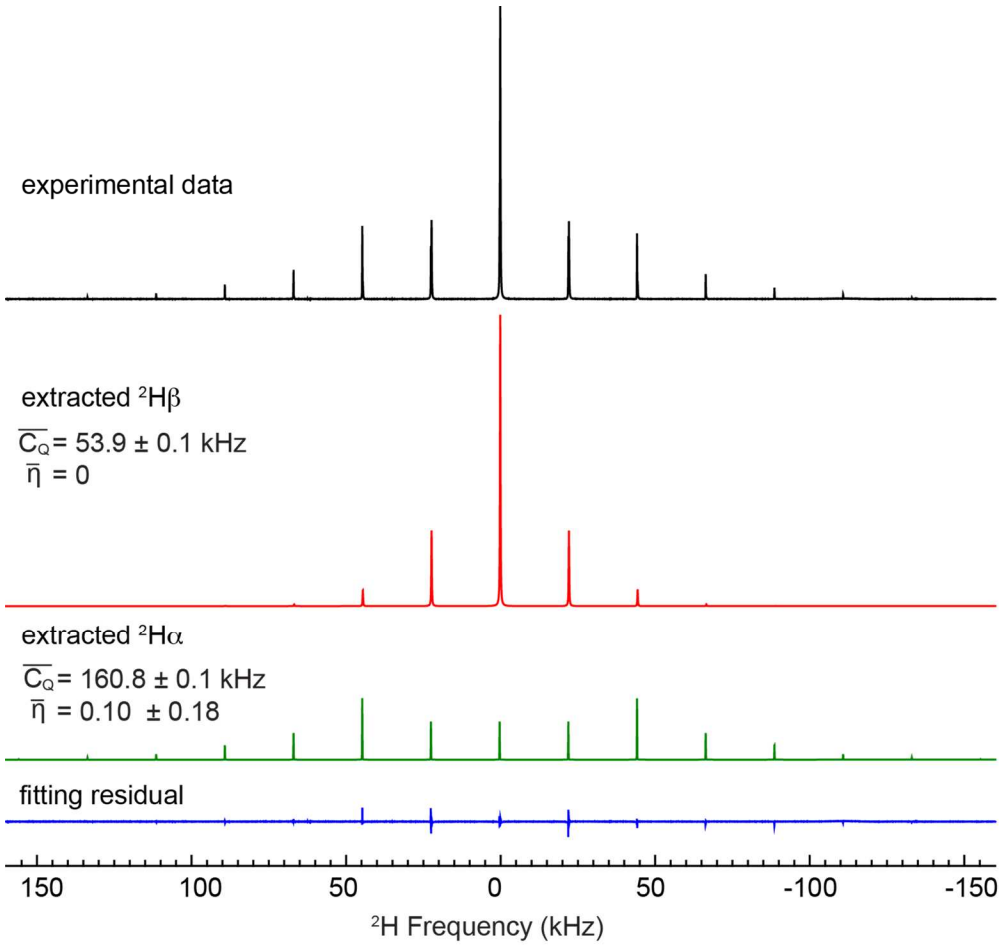

Figure S4. Ala ^{2}H one-pulse MAS spectrum fit. The extracted $\overline{C_Q}$ and $\bar{\eta}$ values were shown in the figure. The large ^{2}Hα $\bar{\eta}$ error is contributed by peak overlap and that centerband and ±1 spinning sidebands are dominated by ^{2}Hβ signal. Data was collected on U-[$^{13}C_3$,$^2H_4$,^{15}N] Ala crystalline powder. The utilized ^{2}H rf field strengths was 86 kHz and MAS frequency was 22.222 kHz. ^{2}Hβ $\bar{\eta}$ was set to zero in the line shape fitting.

Table S1. Ala ^{2}Hα and ^{2}Hβ $\overline{C_Q}$ obtained from ^{2}H-^{13}C adiabatic RESPIRATION CP experiments at various spin-lock rf conditions using pulse sequence shown in Figure S1A. The utilized CP contact time is 1 ms. Asymmetric parameter (η) was set to zero for the fitting of ^{2}Hβ line shapes.

^{2}H, ^{13}C spin-lock rf field strength	^{2}Hα C_Q (kHz)	^{2}Hβ C_Q (kHz)
83 kHz, 77 kHz	161.6	52.8
70 kHz, 66 kHz	162.0	52.9
62 kHz, 55 kHz	163.5	53.0
52 kHz, 44 kHz	162.8	53.4
47 kHz, 33 kHz	160.4	53.6
39 kHz, 22 kHz	161.1	53.9
Literature	160-170[a]	52.0[b]

a. reported for rigid *sp3* C-H deuterium in amino acid residues.[2-5]
b. reported for L−D_3−Ala crystals at -9 °C and 23 °C.[6]

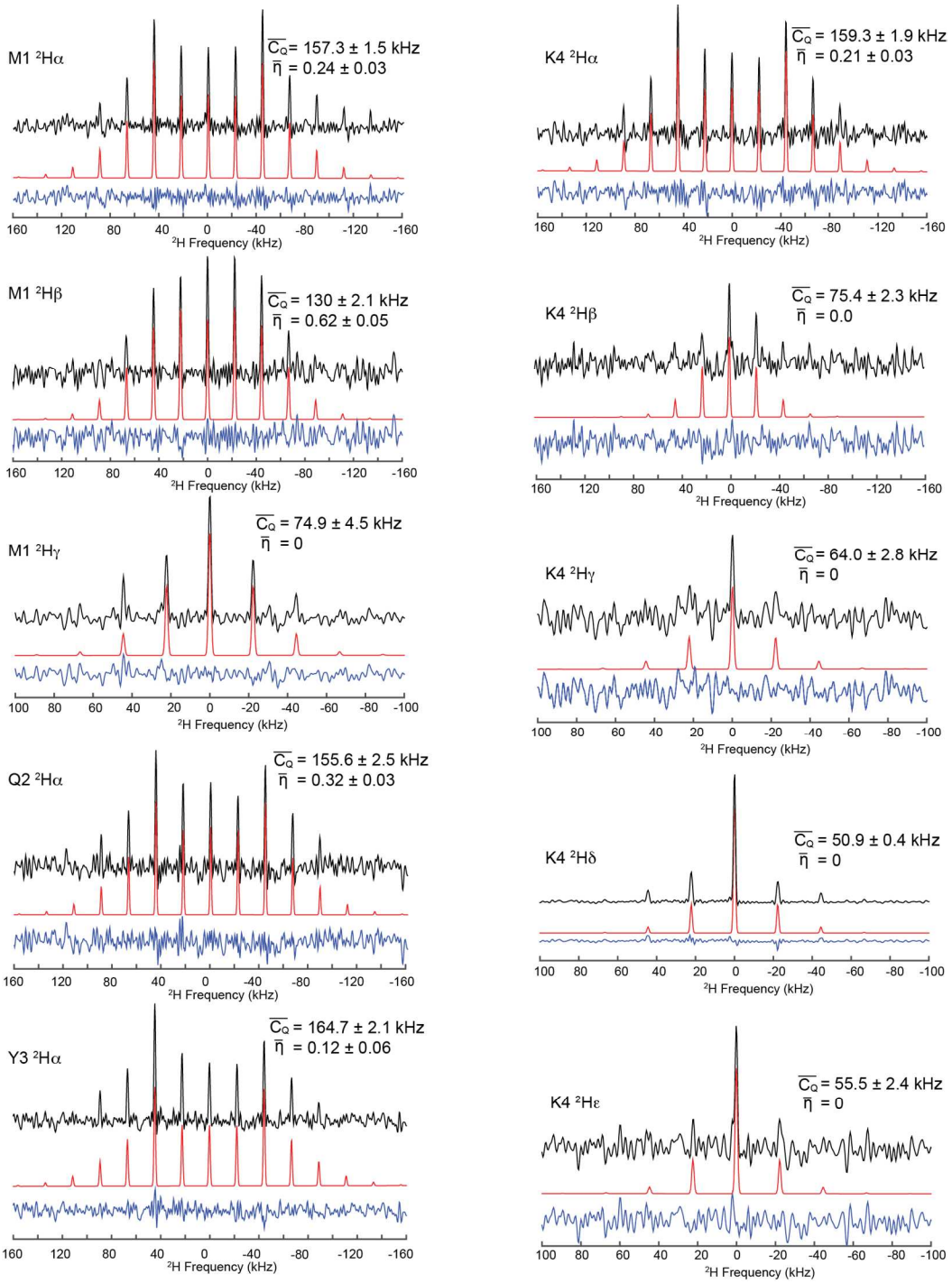

Figure S5. ^{2}H line shape fits for amino acid residues in microcrystalline GB1. Experimental line shapes (black) were extracted from a 3D ^{2}H-^{13}C-^{13}C spectrum. Fits (red) and residuals (blue) are displayed. Fitting was performed using DMFit software[1]. For deuterium undergoing large-amplitude motions, $\overline{\eta}$ was set to zero for the fitting of line shapes. Plots were not shown for deuterium having undetermined line shape due to signal overlap or absence.

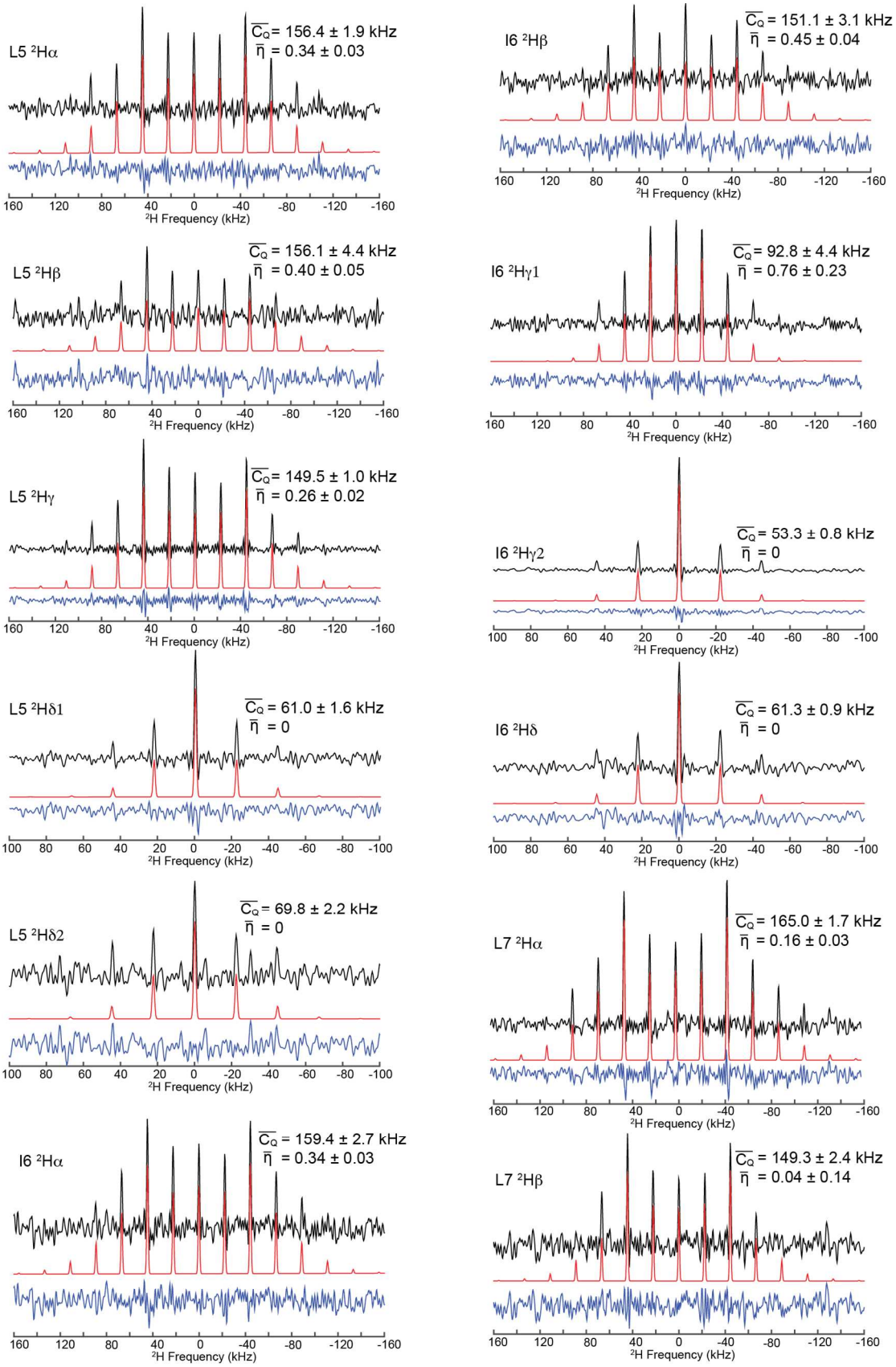

Figure S5 (continued)

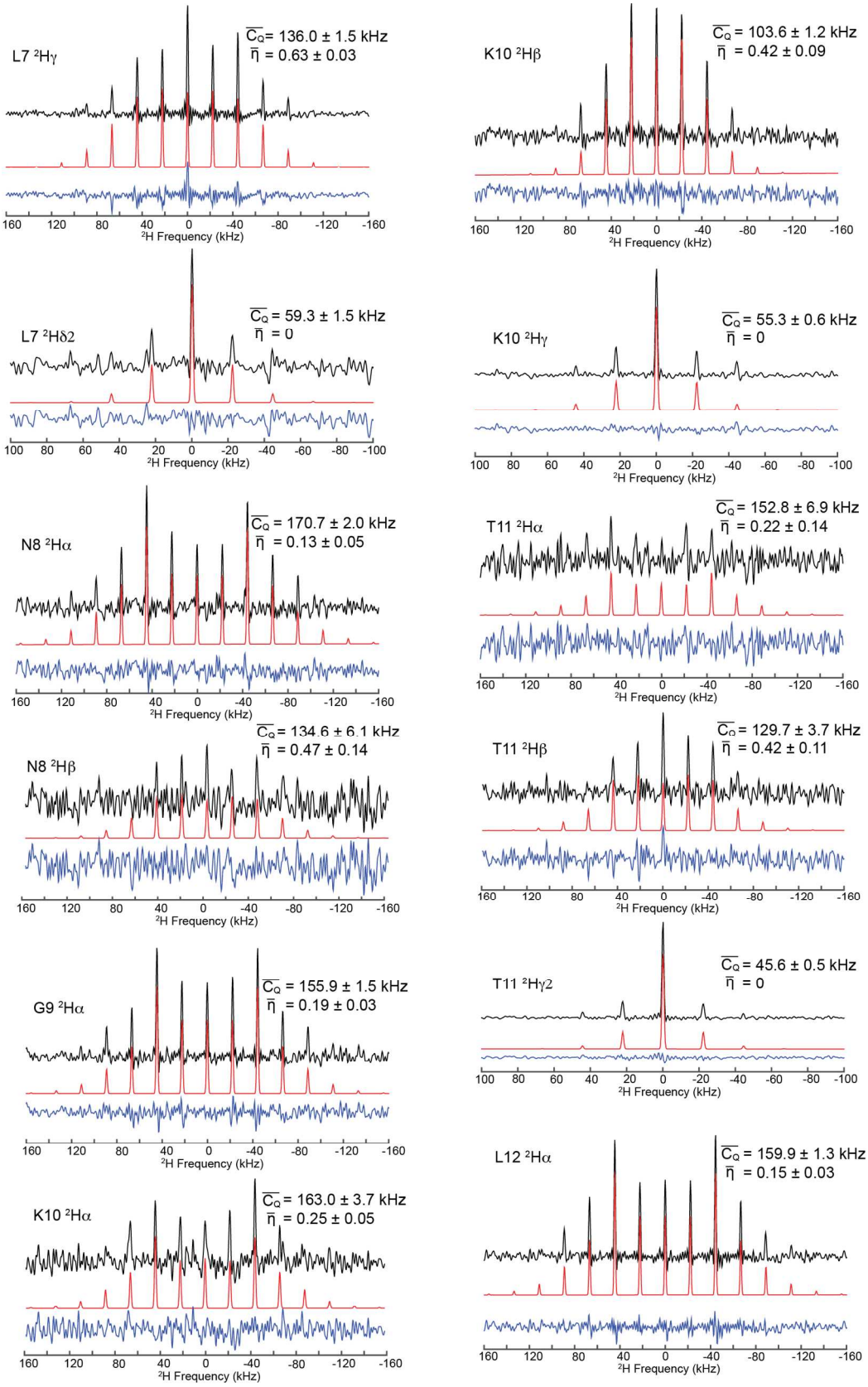

Figure S5 (continued)

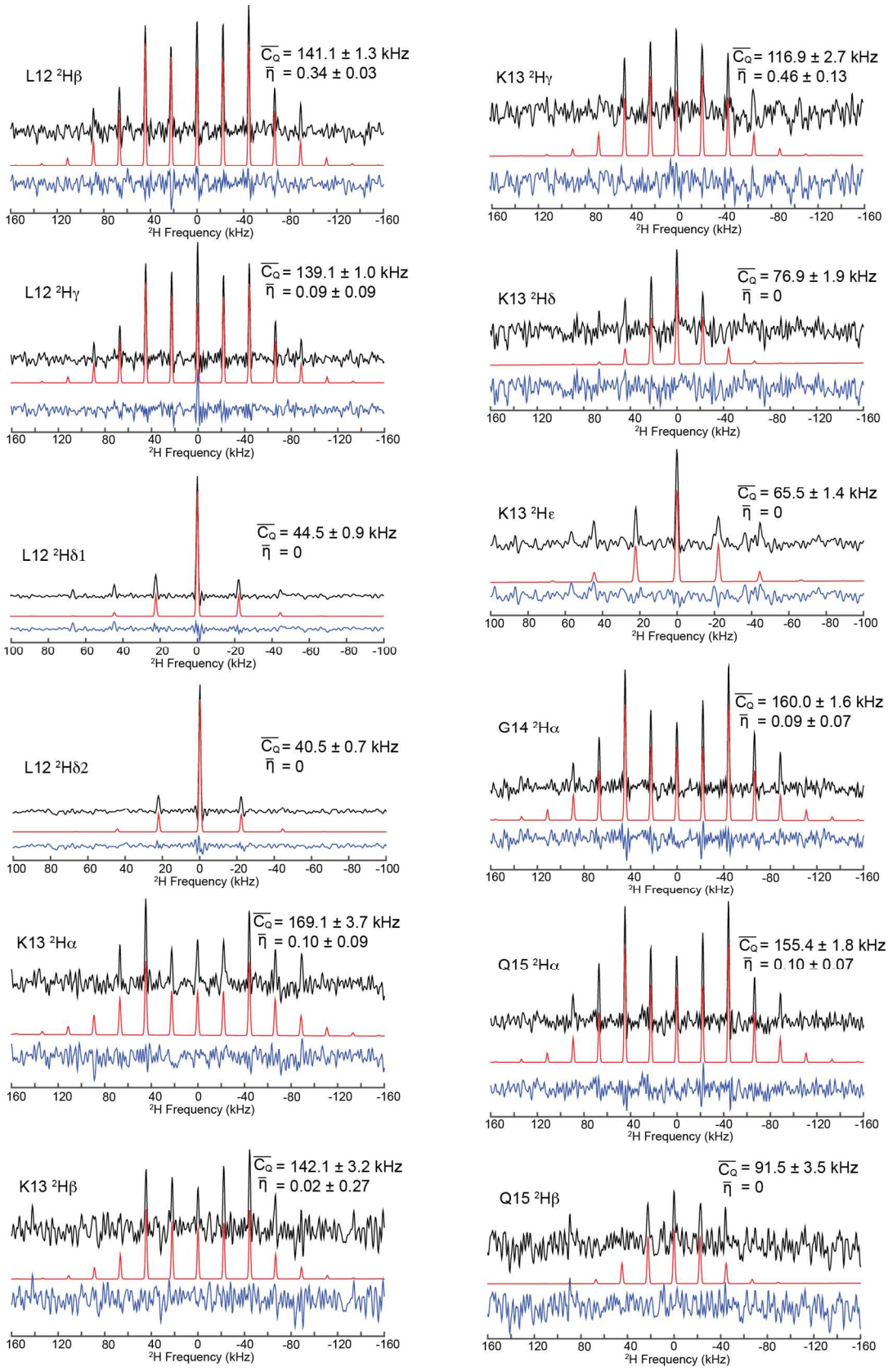

Figure S5 (continued)

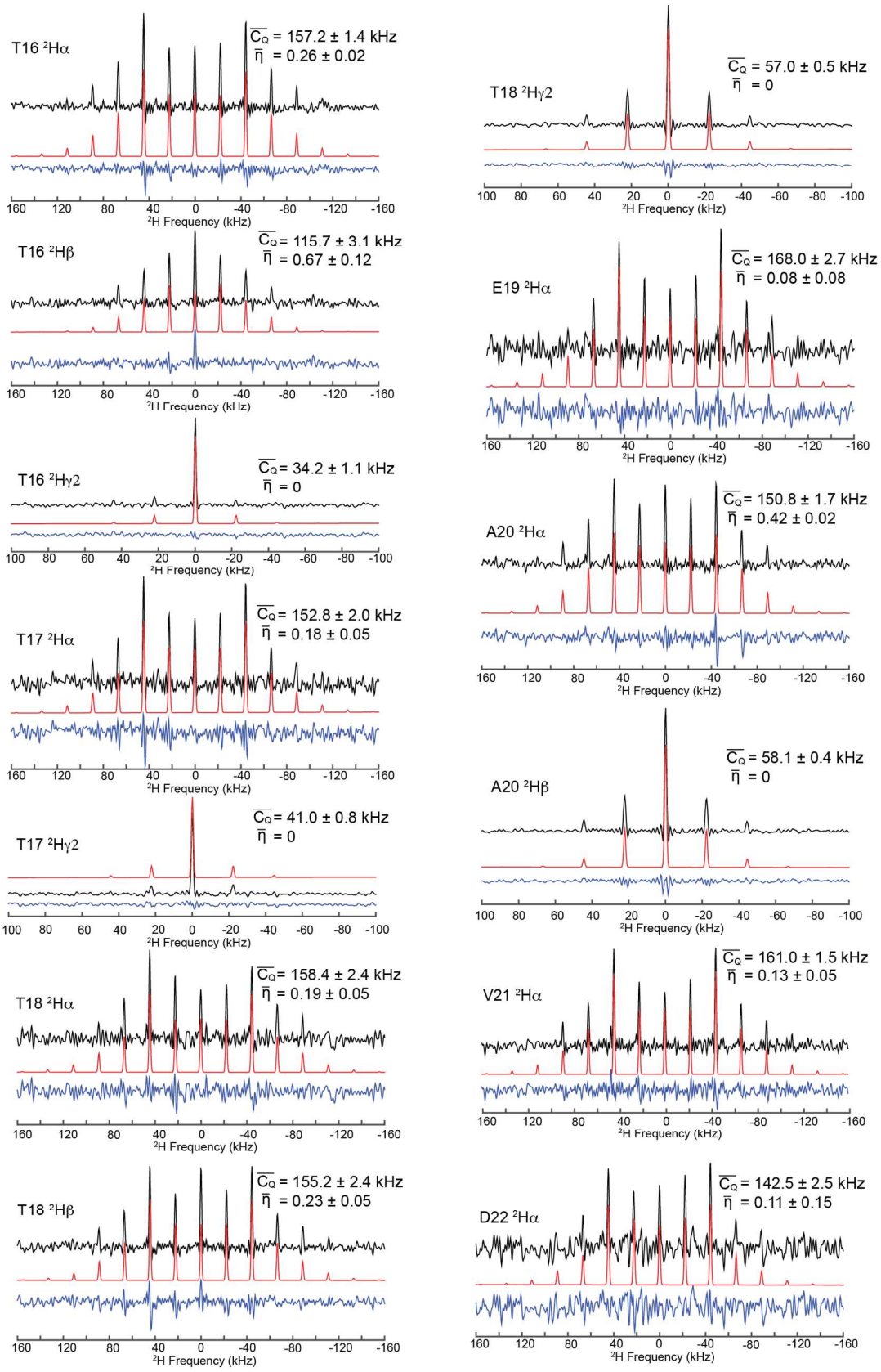

Figure S5 (continued)

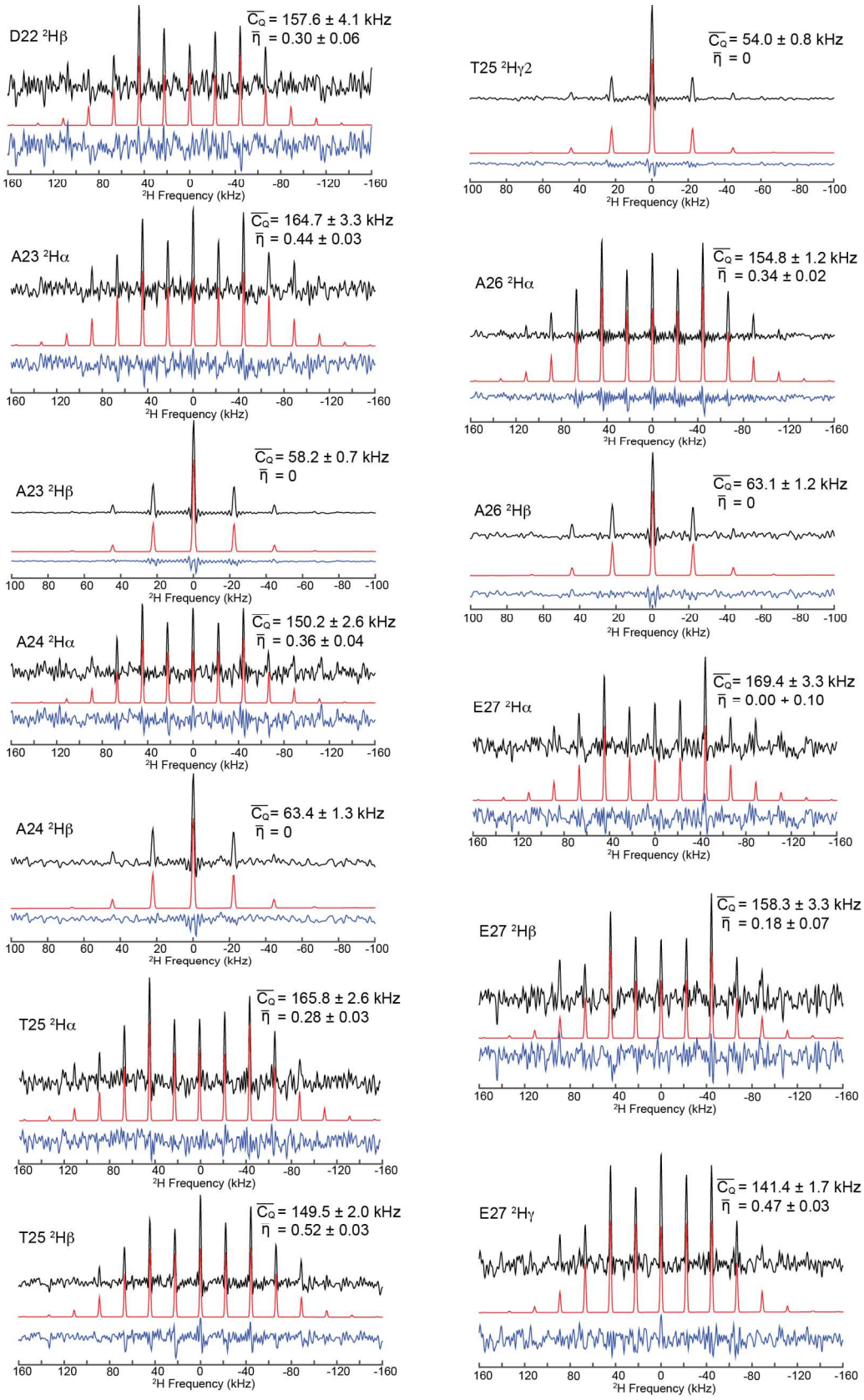

Figure S5 (continued)

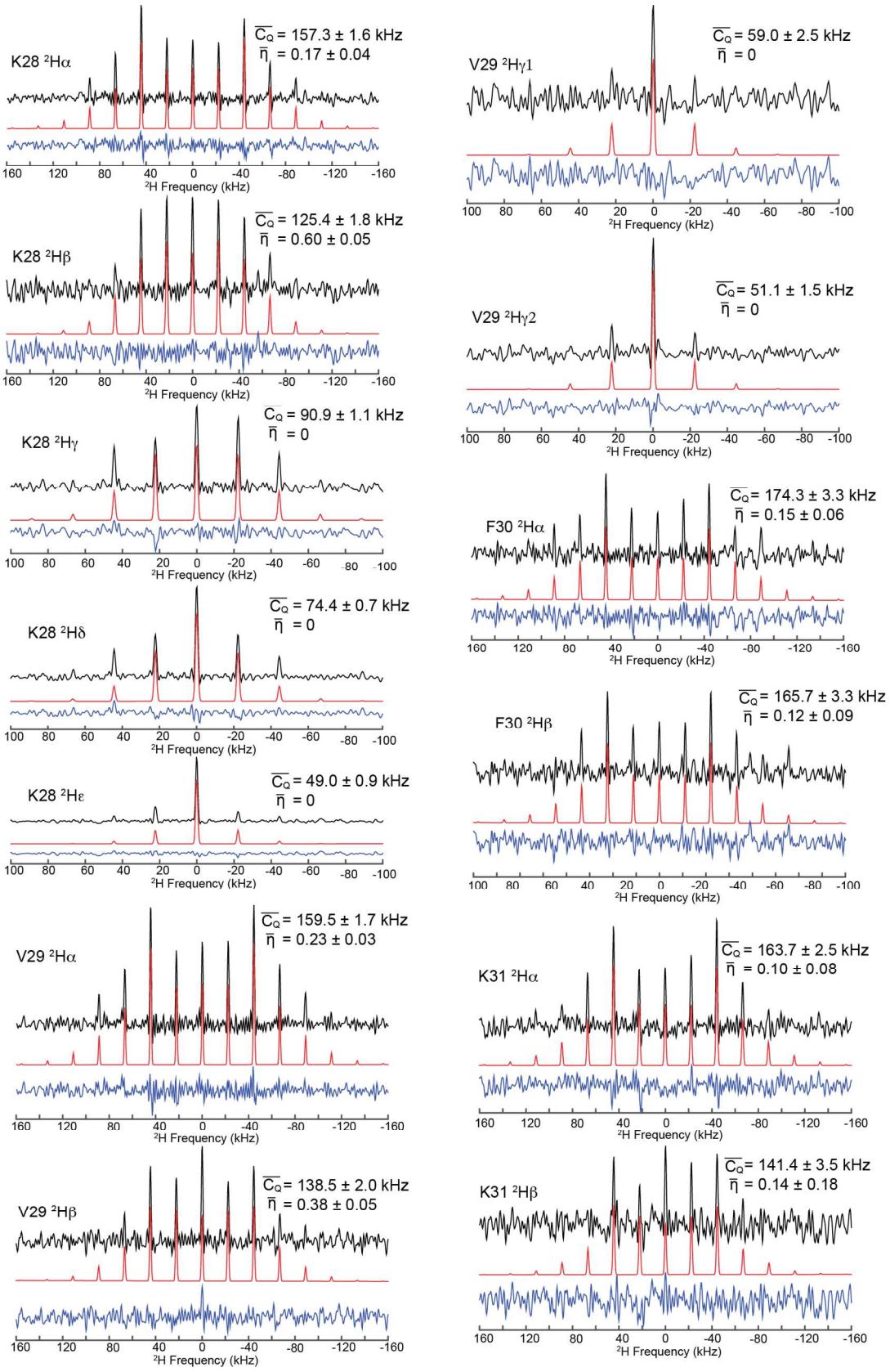

Figure S5 (continued)

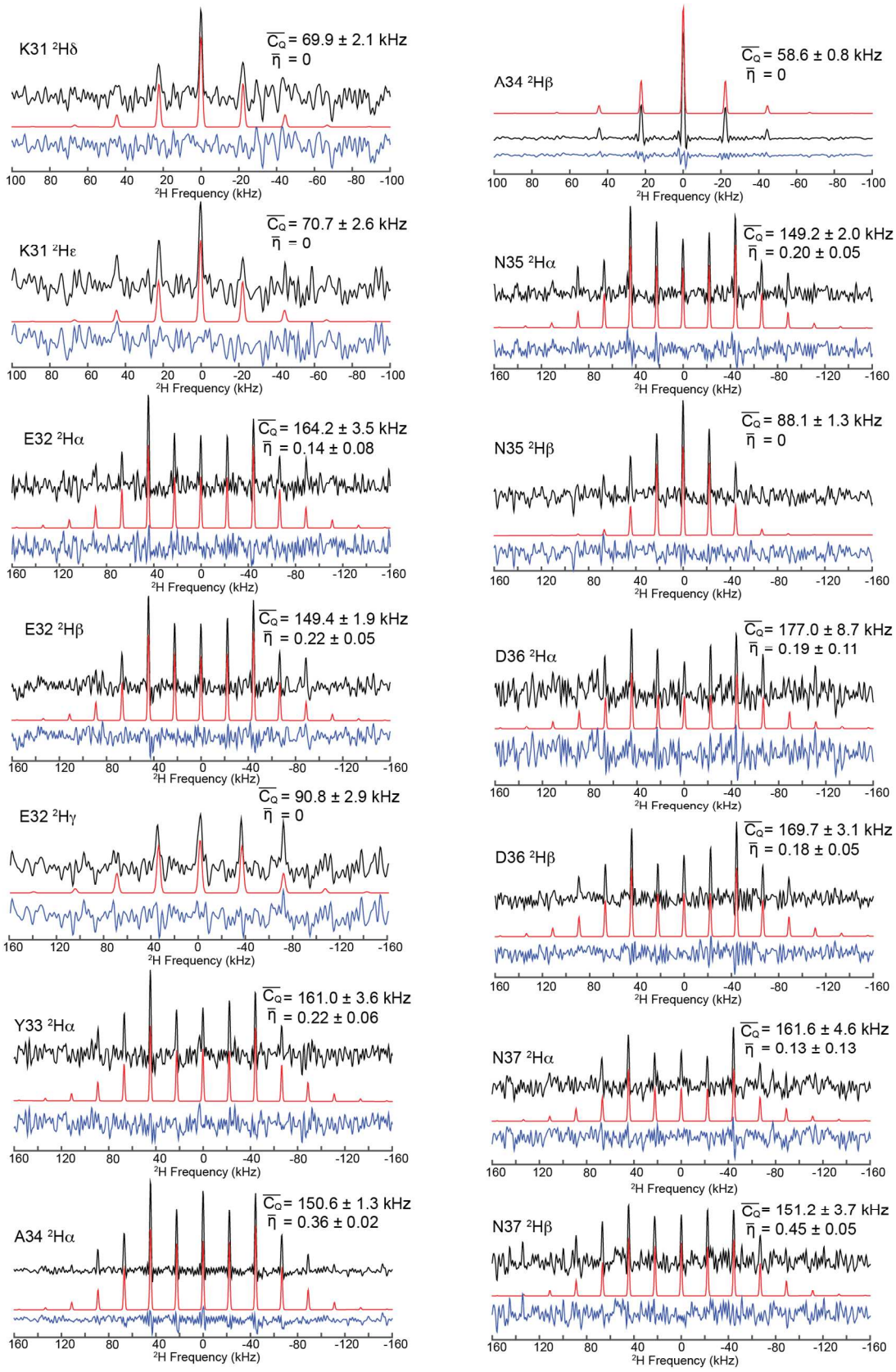

Figure S5 (continued)

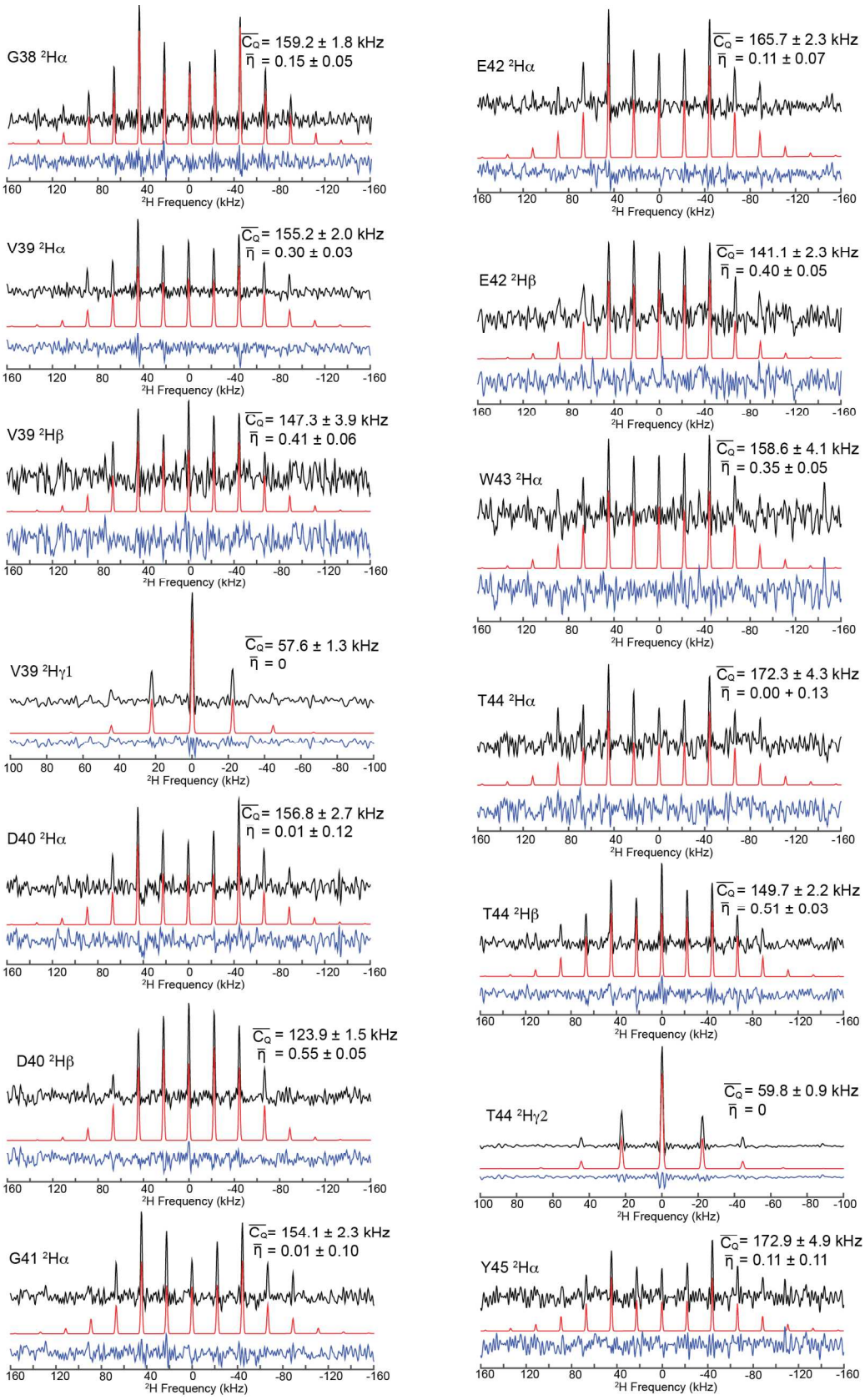

Figure S5 (continued)

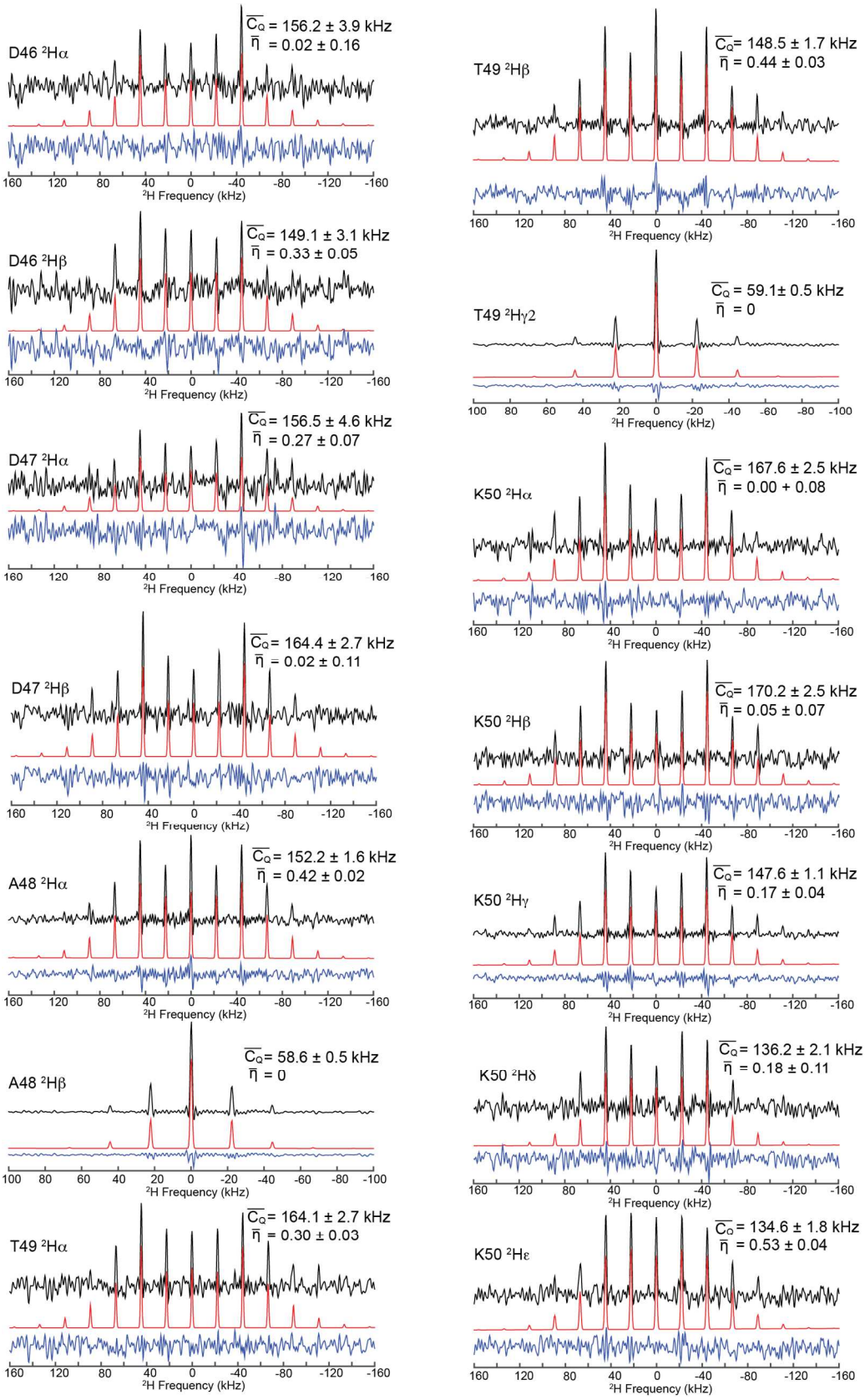

Figure S5 (continued)

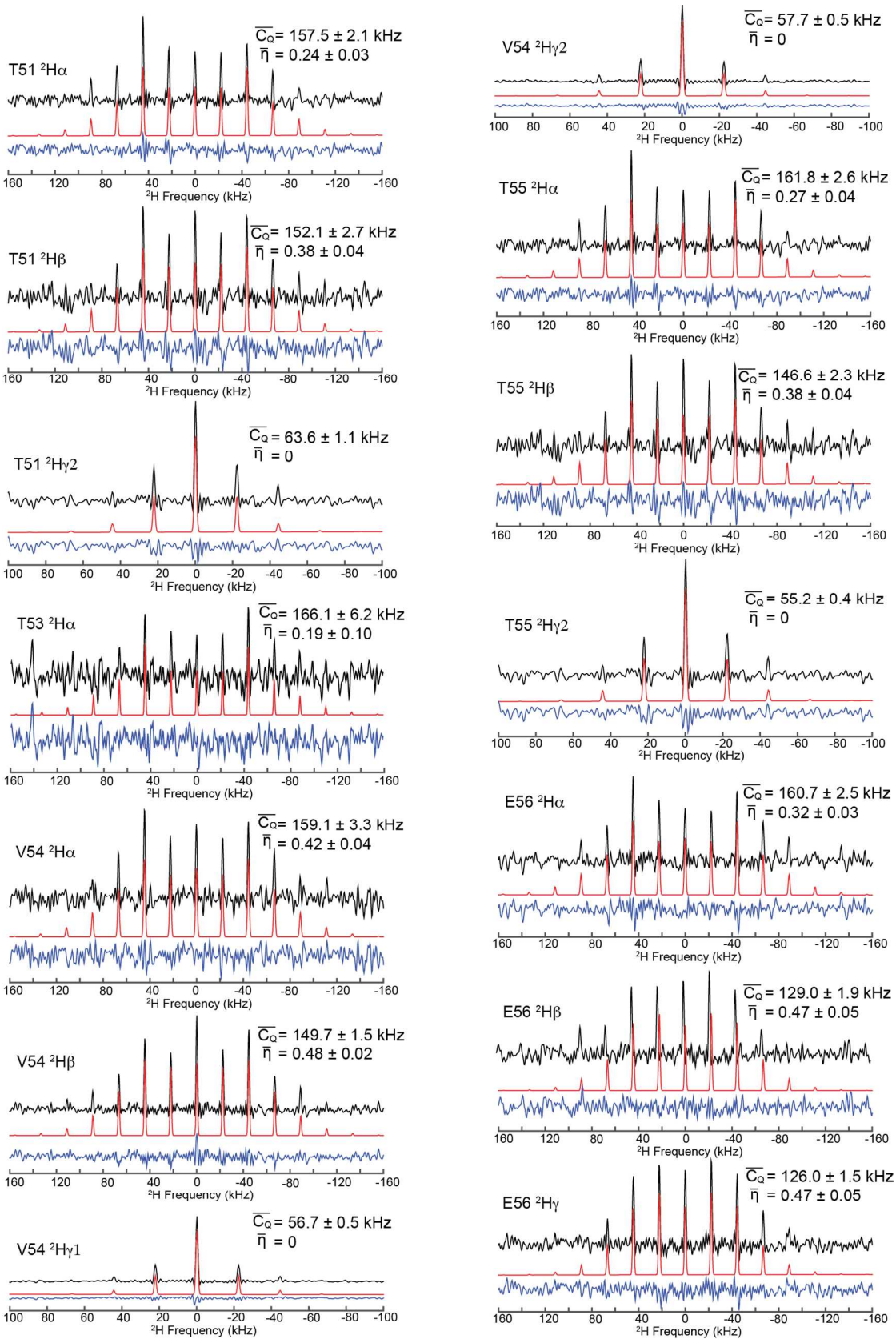

Figure S5 (continued)

Table S2. ^{2}H $\overline{C_Q}$ and $\overline{\eta}$ values determined for Ala aliphatic sites in microcrystalline GB1. For methyl deuterium undergoing large-amplitude motion, $\overline{\eta}$ was set to zero for the fitting of the line shapes.

	^{2}Hα		**^{2}Hβ**	
	$\overline{C_Q}$ (kHz)	$\overline{\eta}$	$\overline{C_Q}$ (kHz)	$\overline{\eta}$
A20	150.8 ± 1.7	0.42 ± 0.02	58.1 ± 0.4	0
A23	164.7 ± 3.3	0.44 ± 0.03	58.2 ± 0.7	0
A24	150.2 ± 2.6	0.36 ± 0.04	63.4 ± 1.3	0
A26	154.8 ± 1.2	0.34 ± 0.02	63.1 ± 1.2	0
A34	150.6 ± 1.3	0.36 ± 0.02	58.6 ± 0.8	0
A48	152.2 ± 1.6	0.42 + 0.02	58.6 ± 0.5	0

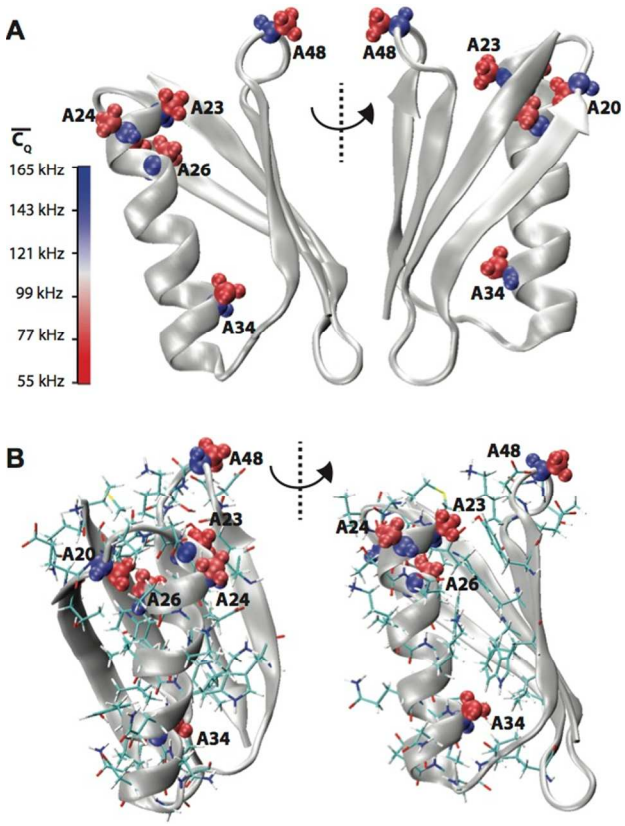

Figure S6. (A) Crystal structure of GB1 (PDB: 2LGI) with Ala aliphatic groups shown in van der Waals spheres and coded with color scaling to $\overline{C_Q}$ values. Two different perspectives are shown for better visualization. (B) Local chemical environment of Ala residues in GB1. The residues having atoms within 5 Å away for the corresponding Ala residue are shown in sticks.

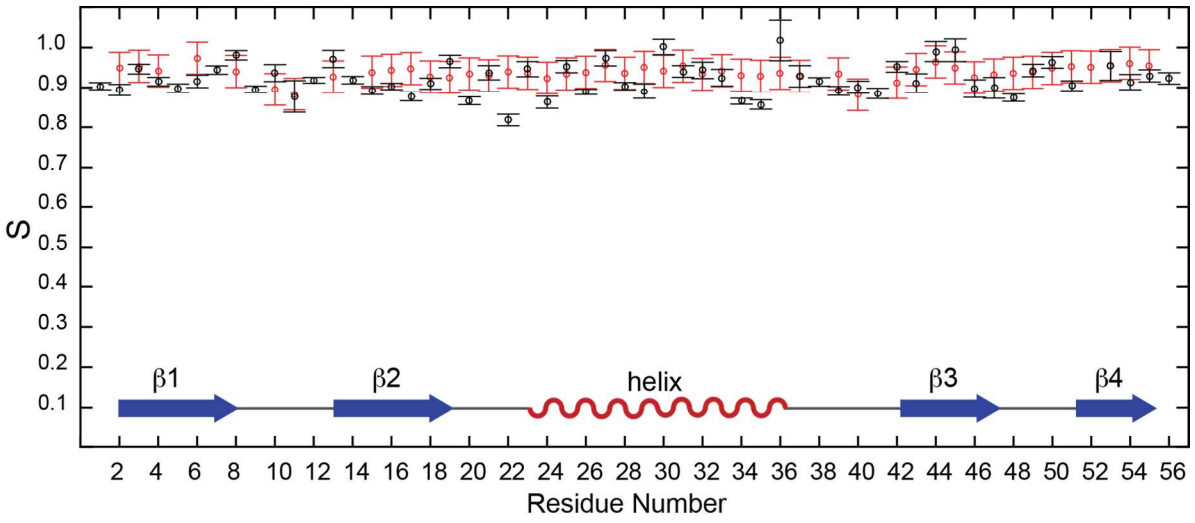

Figure S7. Backbone order parameters derived from ^{2}Hα $\overline{C_Q}/C_Q$(rigid-limit) (black) and dipolar measurement (red) for amino acid residues in microcrystalline GB1. The C_Q(rigid-limit) is assumed to be 174 kHz.[7] The ^{2}Hα $\overline{C_Q}/C_Q$(rigid-limit) value for residue F52 was not determined due to signal overlap. Order parameters from dipolar measurements are from Wylie *et. al*.[8]

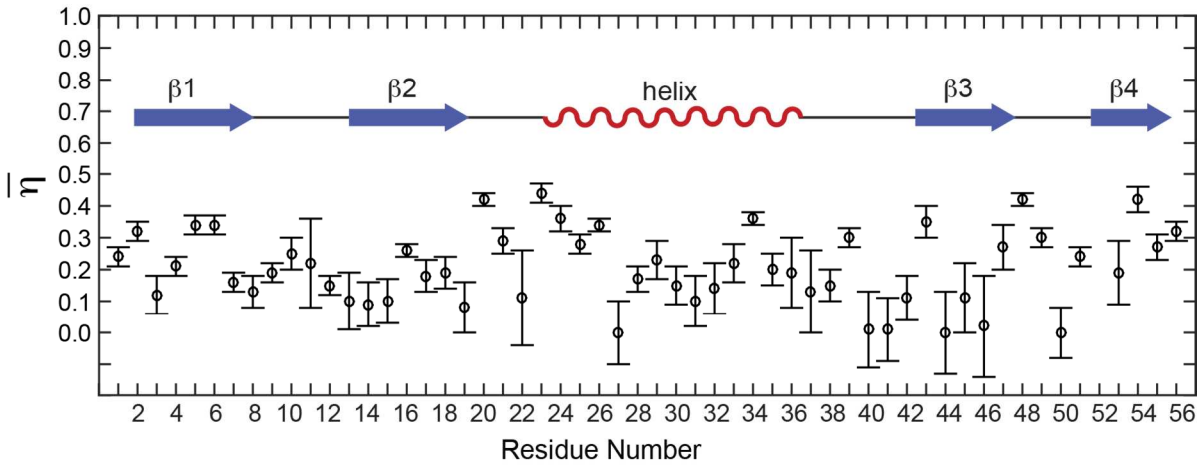

Figure S8. ^{2}Hα $\overline{\eta}$ for amino acid residues in microcrystalline GB1. The value for residue F52 was not determined due to signal overlap. $\overline{\eta}$ values were extracted from ^{2}H line shape fits as represented in Figure S5. $\overline{\eta}$ is greater than or equal to zero by definition. Some error bars were below zero, which were drawn so for the convenience of displaying errors.

REFERENCES

(1) Massiot, D.; Fayon, F.; Capron, M.; King, I.; Le Calve, S.; Alonso, B.; Durand, J. O.; Bujoli, B.; Gan, Z. H.; Hoatson, G. *Magn. Reson. Chem.* **2002**, *40*, 70-76.

(2) Sarkar, S. K.; Young, P. E.; Torchia, D. A. *J. Am. Chem. Soc.* **1986**, *108*, 6459-6464.

(3) Aliev, A. E.; Mann, S. E.; Rahman, A. S.; McMillan, P. F.; Cora, F.; Iuga, D.; Hughes, C. E.; Harris, K. D. *J. Phys. Chem. A* **2011**, *115*, 12201-12211.

(4) Hologne, M.; Faelber, K.; Diehl, A.; Reif, B. *J. Am. Chem. Soc.* **2005**, *127*, 11208-11209.

(5) Shi, X.; Yarger, J. L.; Holland, G. P. *J. Magn. Reson.* **2013**, *226*, 1-12.

(6) Batchelder, L. S.; Niu, C. H.; Torchia, D. A. *J. Am. Chem. Soc.* **1983**, *105*, 2228-2231.

(7) Sheppard, D.; Li, D. W.; Bruschweiler, R.; Tugarinov, V. *J. Am. Chem. Soc.* **2009**, *131*, 15853-15865.

(8) Wylie, B. J.; Sperling, L. J.; Nieuwkoop, A. J.; Franks, W. T.; Oldfield, E.; Rienstra, C. M. *Proc. Natl. Acad. Sci. U S A* **2011**, *108*, 16974-16979.